



# Particle Acceleration due to Magnetically Driven Reconnection using Laser-Powered Capacitive Coils

Geoffrey Pomraning<sup>1</sup>, Lan Gao<sup>2</sup>, and Hantao Ji<sup>1,2</sup>

1) Princeton University, 2) Princeton Plasma Physics Laboratory



## Abstract

Magnetic Reconnection is the ubiquitous astrophysical process in which a plasma rapidly converts magnetic field energy into a combination of flow energy, thermal energy and non-thermal energetic particles. Various acceleration mechanism (including Fermi acceleration, betatron acceleration, parallel electric field acceleration and out-of-plane electric field acceleration) have been theoretically proposed and numerically studied in collisionless low- $\beta$  environments. Only recently [1] has this environment been experimentally studied using the Omega-EP platforms. By using kJ lasers, we drive parallel currents through capacitive coil targets to achieve MegaGauss-level magnetic reconnection. We summarize results indicating that the primary acceleration mechanism in this setup is the out-of-plane reconnection electric field. We then present further laser-target reconnection concepts that will allow us to both verify these results and directly study alternative particle acceleration mechanisms.

## Experimental Setup

Figure 1 shows the experimental setup of magnetic reconnection experiments using capacitor coil with two major diagnostics. OMEGA-EP long-pulse beams pass through the front holes and irradiate the back plate delivering a combined -2.5 kJ in 1 ns. An electrostatic potential is induced between the (capacitive) plates and a large (-40-70 kA) current is driven through the parallel U-shaped coils. The resulting magnetic fields undergo reconnection between the coils. One diagnostic is the OU-ESM, positioned 37.5 cm away from the main interaction at an angle of 39° away from the vertical. Five independent channels (directions indicated with the solid cyan lines above) are spaced 5° apart, allowing the direct measurement of angular spread of electrons in the azimuthal direction. The other diagnostic is a 2 $\omega$  (527 nm) Thomson scattering beam which probes the exhaust region 600  $\mu$ m above the center point at the top of the coils. The scattered light volume of 60 x 60 x 50  $\mu$ m<sup>3</sup> is collected by an f/10 reflective collection system.

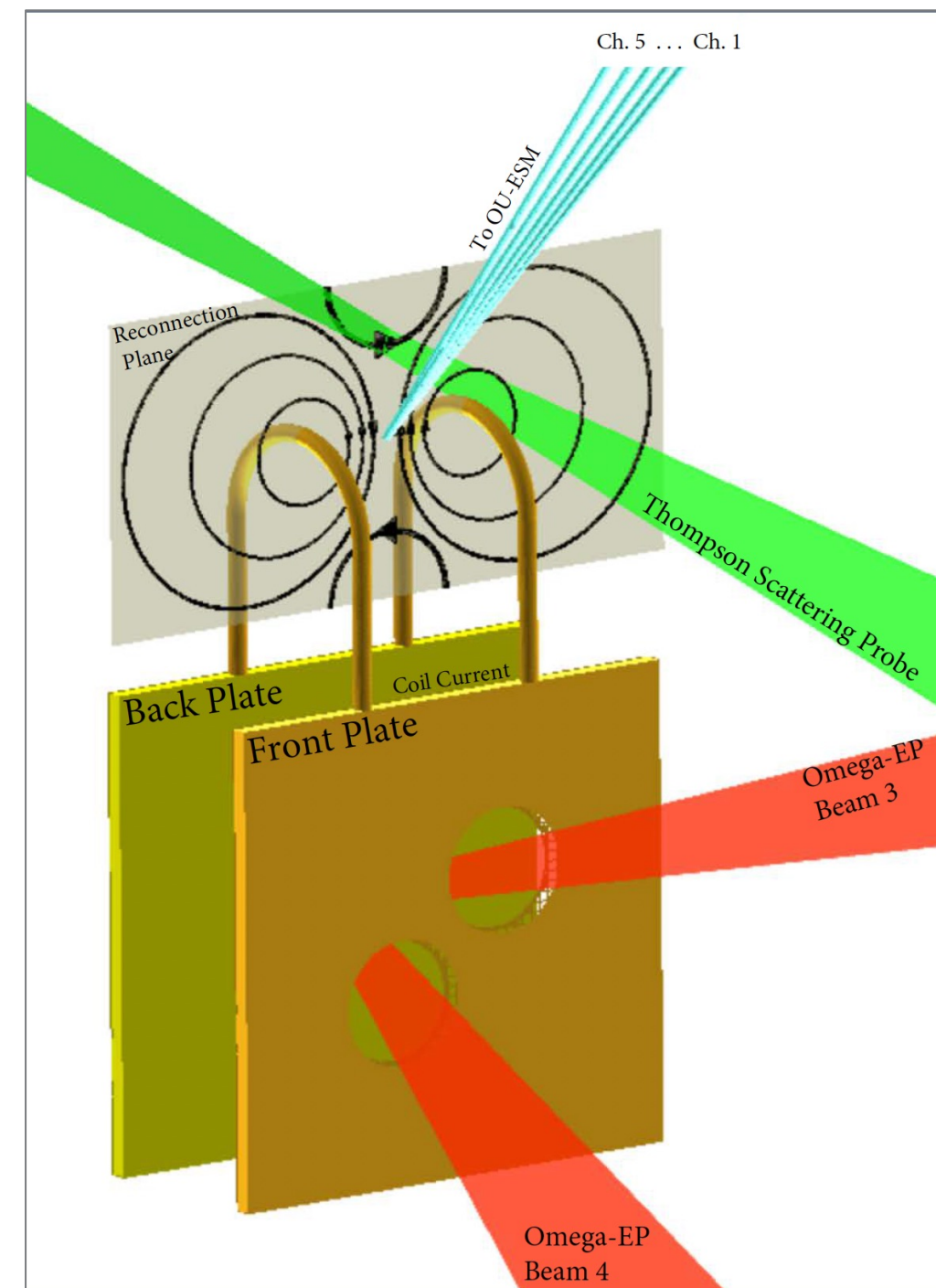


Figure 1: A schematic diagram of the capacitively coupled target ion Omega-EP. Note particularly the OU-ESM diagnostic used for taking data for our experiment. [3]

## Simulation and Acceleration Mechanisms

In this procedure a strong magnetic field is generated between the capacitive coils of our setup. Reconnection occurs at the interface of the two coils in a central plane. Experimental data is compared to simulations

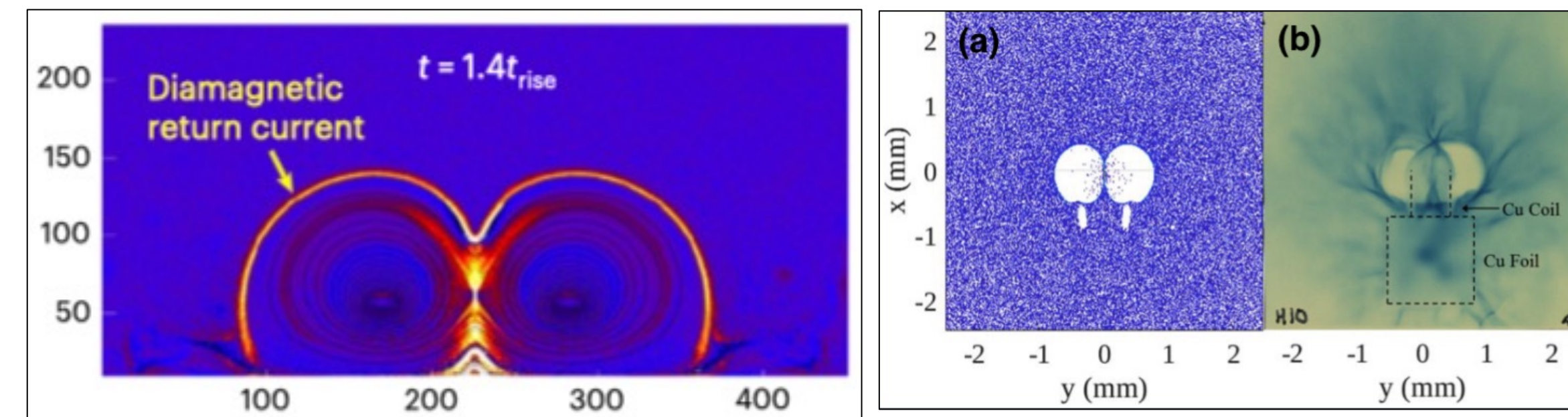


Figure 2: A diagram of the laser induced magnetic field from simulation. This synthetic reconstruction emphasizes the central reconnection feature and can be compared to Figure 3. Reproduced from [4]

Figure 3: (a) another synthetic radiograph, this time showing the prolate voids (b) the achieved magnetic field from the capacitive coil. Note both the void structure and the central feature for the reconnection [2]

We further validate the physicality of interest for our experiment by comparing parameter regimes which our experiment can access

Platform	RHESSI	MMS	MRX/FLARE	Capacitor Coil=micro-MRX
Location	Solar	Space	Lab	Lab
Regime	e/ion	e/ion	e/ion	electron only
Ion	H	H	H	Cu <sup>+</sup> (Z = 18)
Length Scale L <sub>0</sub>	10 <sup>4</sup>	≈ 10 <sup>4</sup>	0.8 → 1.6m	1 mm
Current Sheet 2L <sub>CS</sub>	10 <sup>4</sup>	≈ 10 <sup>4</sup>	0.4 → 0.8m	300 $\mu$ m
e <sup>-</sup> Density n <sub>e0</sub>	10 <sup>11</sup> cm <sup>-3</sup>	≈ 1.1 cm <sup>-3</sup>	10 <sup>13</sup> cm <sup>-3</sup>	10 <sup>18</sup> cm <sup>-3</sup>
System Size $\lambda = \frac{L_0}{v_A}$	≈ 10 <sup>3</sup>	10 <sup>3</sup>	11	≈ 5.2
T <sub>e</sub>	100eV	100 – 1000eV	10 – 30eV	300eV
Magnetic field B	.02T	20 – 100nT	.03T	100T
Plasma Beta $\beta$	.01	.04 – .6	.09	≈ .06
Lundquist Number S	10 <sup>13</sup>	10 <sup>14</sup>	< 10 <sup>3</sup>	1.82 · 10 <sup>2</sup>
e <sup>-</sup> Mean Free Path	10 <sup>2</sup> m	10 <sup>4</sup> → 10 <sup>5</sup> m	5cm (<< L <sub>0</sub> )	55 $\mu$ m
Control	No	No	Yes	Yes
In-situ measurement	No	Yes	difficult	No
Ex-situ measurement	Yes	No	No	Yes

Figure 4: An illustrative table comparing the regimes that this experiment can access to other astrophysically relevant regimes and reconnection experiments. [3]

## Experimental Results and Validation

To fully understand our experimental results, we first consider the possible acceleration mechanisms in magnetic reconnection. Namely, we consider Fermi, Betatron, direct electric field and cross B field acceleration

$$\frac{d\epsilon}{dt} = qE_{\parallel}v_{\parallel} + \mu \frac{dB}{dt} + q\mathbf{E} \cdot \mathbf{u}_c + \frac{1}{2} m \frac{d}{dt} |\mathbf{u}_E|^2$$

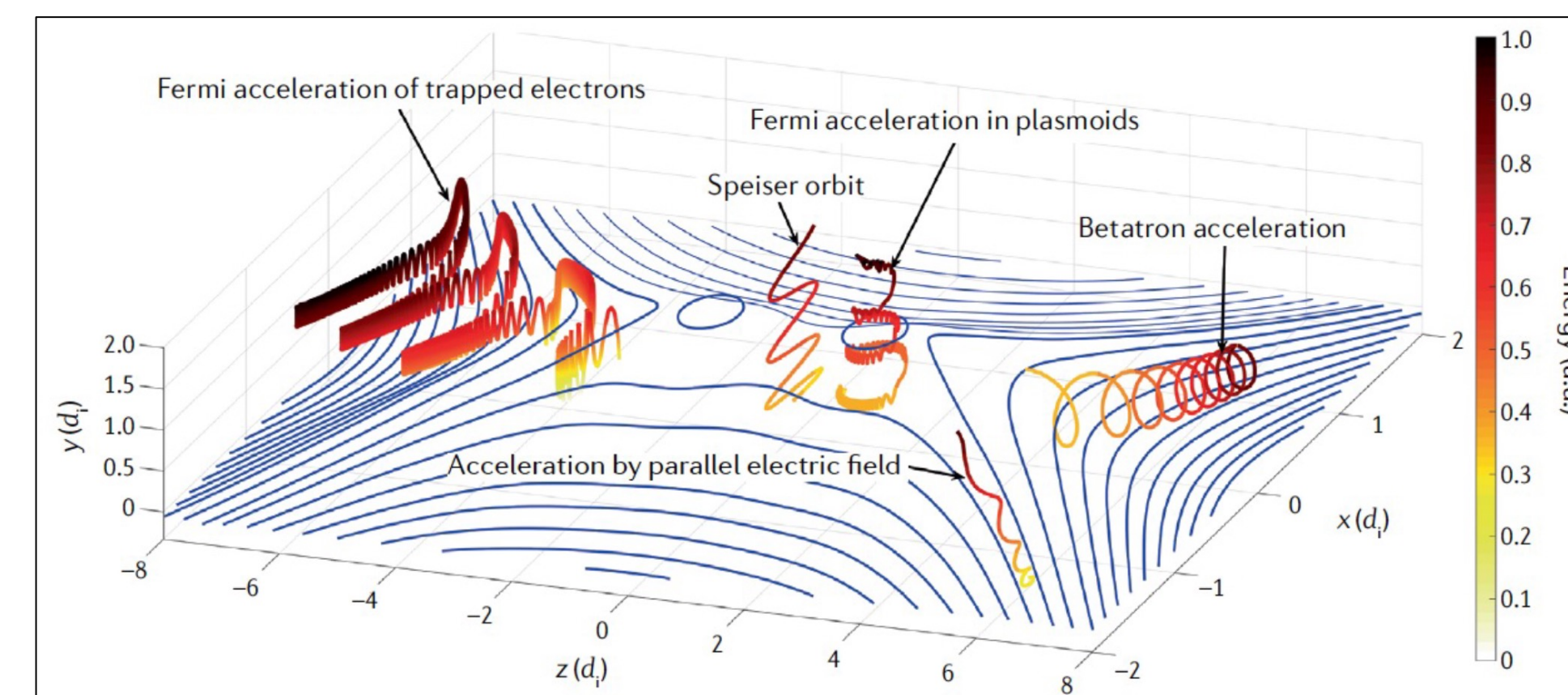


Figure 5: An equation showing various particle acceleration terms and a diagram illustrating the differences in types of magnetic reconnection accelerations. Here  $\mathbf{u}_c$  is velocity from curvature drift and  $\mathbf{u}_E$  is ExB drift velocity. We note that by measure quantities in our experiment, we can determine the relative contribution of each term and therefore each mechanism in our experiment. [5]

Experimental results we then obtained from the electron energy profiles measured by the OU-ESM. In particular, we note that “reconnection bumps” appeared in our analysis, which allow us to determine the predominant sources of particle acceleration in our experiment

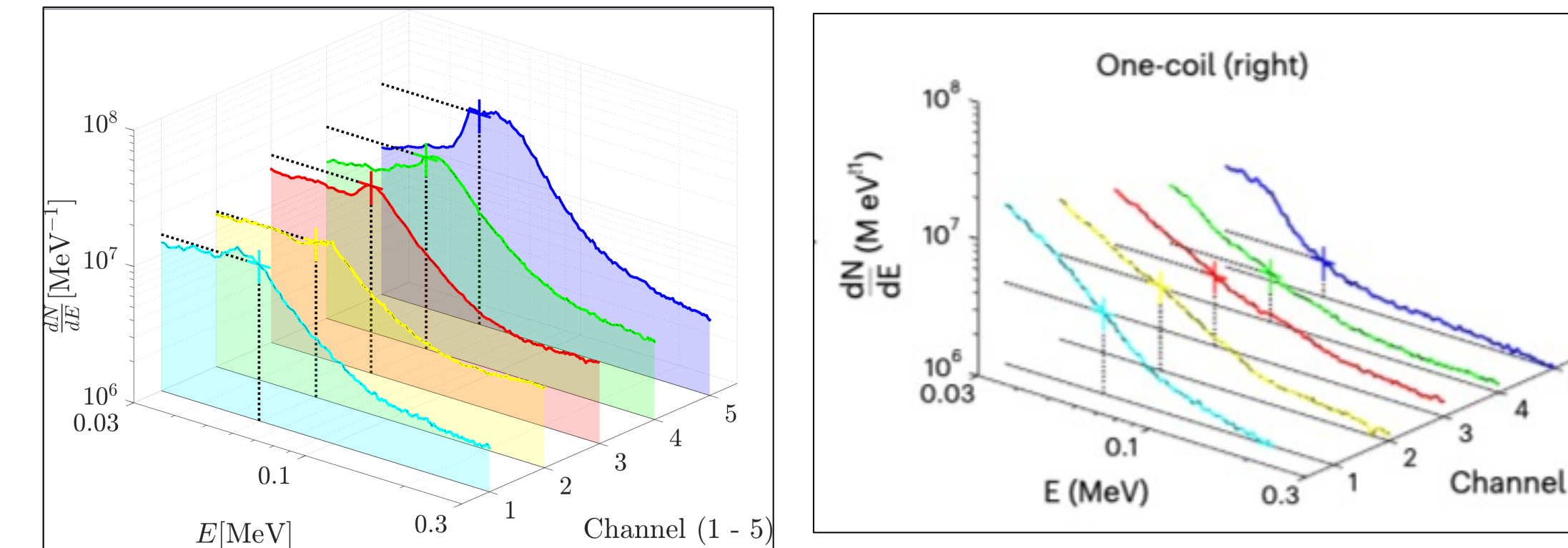


Figure 6: Electron distributions from laser experiments. Here we note that the “bump” feature appears in all channels when our experiment undergoes reconnection (left) but does not appear at all when only a single coil is placed in our target (right). Thus, we conclude this non-Maxwellian bump must be due to reconnection. To use this distribution to get an estimate of the primary acceleration mechanisms, we leverage experimental data to estimate of the reconnection electric field from the Alfvén speed and reconnection rate. Taking a characteristic acceleration distance in our experiment, we find electric field acceleration contributes approximately at the peak in energy we see. A more complete analysis of this procedure and other acceleration mechanisms is available in [1,3]

## Further Extensions

Further extensions of this work have been proposed. Preliminary analysis indicates that using short pulse lasers to drive higher reconnection magnetic fields yields similar results, giving additional verification of the dominance of out-of-plane electric field acceleration. We further propose new experiments that will allow us to study plasmoid instability and turbulence mechanisms due to Fermi acceleration.

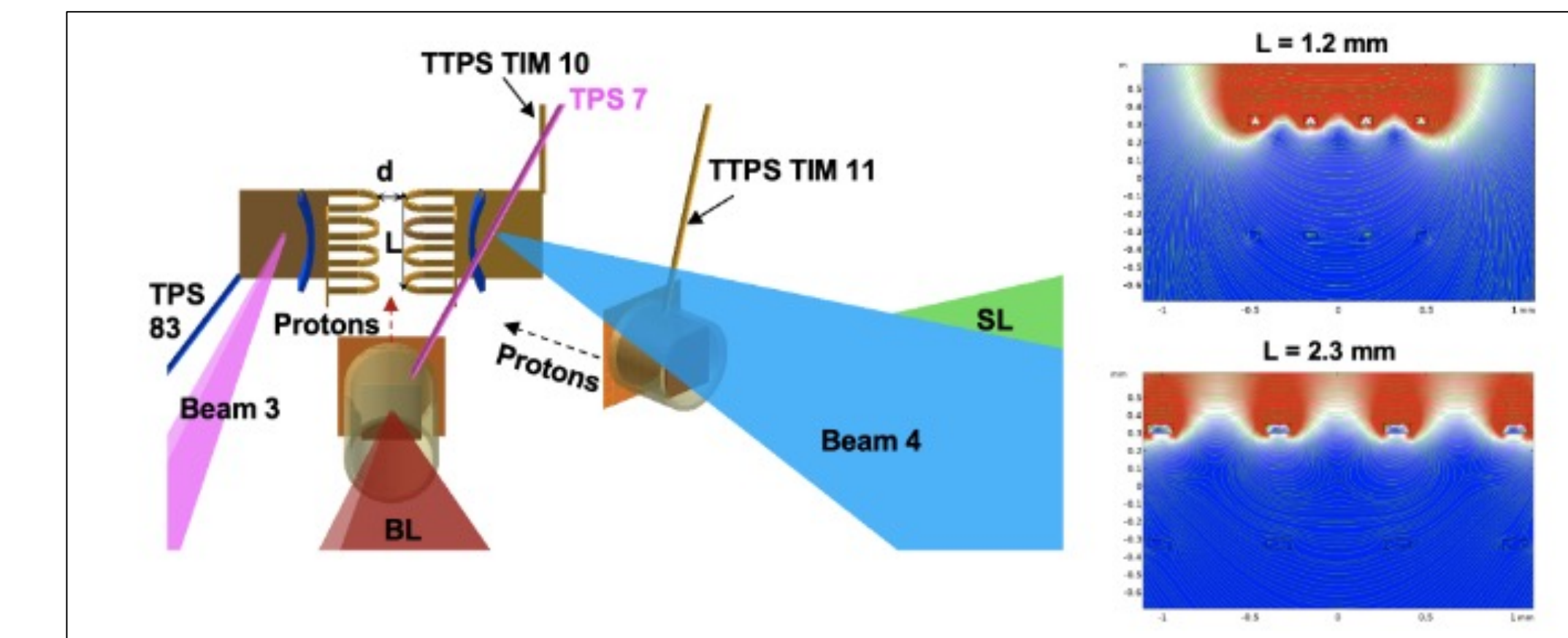


Figure 7: A sample new experimental setup to examine Fermi accelerated electrons. By changing the current sheet lengths, we will be able to vary the formation of the plasmoids in these sheets, and therefore distinguish and study individual acceleration mechanisms. Promising preliminary simulations indicate plasmoids can form in these conditions.

## Conclusion

Laser-Driven capacitive coils offer an exciting new platform to study astrophysically relevant magnetic reconnection. Preliminary analysis has allowed us to determine the primary mechanism of this acceleration as direct electric field acceleration and new target design will allow us to explore other reconnection particle acceleration mechanisms in the lab.

## Acknowledgements

This work was supported Princeton University and the Princeton Plasma Physics Laboratory with support from FES, USDOE, and LLE’s OMEGA facility.

## References

- [1] A. Chien, L. Gao, S. Zhang, H. Ji, E. Blackman, W. Daughton, A. Stanier, A. Le, F. Guo, R. Follett, H. Chen, G. Fiksel, G. Bleotu, R. Cauble, S. Chen, A. Fazzini, K. Filippo, O. French, D. Froula, J. Fuchs, S. Fujioka, K. Hill, S. Klein, C. Kuranz, P. Nilson, A. Rasmus, R. Takizawa, “Non-thermal electron acceleration from magnetically driven reconnection in a laboratory plasma,” *Nature Physics* **19**, 254 (2023)
- [2] A. Chien, L. Gao, H. Ji, X. Yuan, E. G. Blackman, H. Chen, P. C. Efthimion, G. Fiksel, D. H. Froula, K. W. Hill, K. Huang, Q. Lu, J. D. Moody, and P. M. Nilson, “Study of a magnetically driven reconnection platform using ultrafast proton radiography,” *Phys. Plasmas* **26**, 062113 (2019)
- [3] H. Ji, L. Gao, A. Chien, S. Zhang, E. Blackman, G. Pomraning, K. Sakai, F. Guo, X. Li, and A. Stanier “Study of magnetic reconnection at low- $\beta$  using laser-powered capacitor coils” [Manuscript in Preparation] (2023)
- [4] S. Zhang, A. Chien, L. Gao, H. Ji, E. Blackman, R. Follett, D. Froula, J. Katz, C. Li, A. Birkel, R. Petrasso, J. Moody, and H. Chen, “Ion and Electron Acoustic Bursts during Anti-Parallel Reconnection Driven by Lasers,” *Nature Physics* **19**, 909 (2023)
- [5] H. Ji, W. Daughton, J. Jara-Almonte, A. Le, A. Stanier, and J. Yoo, “Magnetic reconnection in the era of exascale computing and multiscale experiments,” *Nature Reviews Physics* **4**, 263 (2022)